

April 1, 2025
Determining Bravais Lattice Types

LAWRENCE C. ANDREWS,^{a*} HERBERT J. BERNSTEIN^b AND NICHOLAS K. SAUTER^c

^a*9515 NE 137th St, Kirkland, WA, 98034-1820 USA,* ^b*c/o NSLS-II, Brookhaven National Laboratory, Upton, NY, 11973 USA, Rochester Institute of Technology, c/o NSLS-II, Brookhaven National Laboratory, Upton, NY, 11973 USA, and ^cLawrence Berkeley National Laboratory, 1 Cyclotron Rd., Berkeley, CA, 94720 USA.*

E-mail: larry6640995@gmail.com

Unit cell reduction; Delaunay; Delone; Niggli; Selling; Bravais Lattice

Abstract

We introduce a new Bravais lattice determination algorithm. SELLA is a straightforward algorithm and a program for determining Bravais lattice type based on Selling (Delone) reduction. It provides a clear metric of fit to each type. The mathematical foundations for treating near-symmetries are described. The 24 Bravais lattice types described by Delaunay (1932) are described as linear manifolds in 6-dimensions.

1. Introduction

We introduce a new Bravais lattice determination algorithm. The Bravais lattice types were created by Bravais (1850). Delaunay (1932) and Niggli (1928) developed methods for the identification of the Bravais lattice type of a crystal using the measured

unit cell dimensions; their methods were exact only if the cell parameters exactly corresponded to the actual type (Patterson & Love, 1957). Delaunay (Delaunay, 1932) discussed the issues of scalars that have nearly zero values, but the broader issues of measurement errors were not discussed. (Delaunay later changed the spelling to Delone, a transliteration of the Cyrillic spelling of his name.)

Zimmermann & Burzlaff (1985) described the program, DELOS for the same purpose and based on the use of Selling scalars, which SELLA uses as well; they treat the scalars as a list of 6 numbers, but do not consider them as points in a space. SELLA treats the scalars as elements of vectors in the 6-dimensional space, \mathbf{S}^6 . Treating lattices as points in a liner space accesses the tools and systematic procedures of linear algebra.

Andrews & Bernstein (2014) reviewed the literature on efforts to create methods to utilize data that contain unavoidable measurement error and adds a more generic view of the problem.

SELLA is a based on Selling (Delone) reduction. It is a complete, closed solution, and it provides a clear metric of fit to each type.

2. Terminology

2.1. The Bravais types

Delaunay (1932) found that the 14 Bravais lattice types could be allocated among 24 types that are determined by the type of Dirichlet unit cell (termed the Voronoi region (Voronoi, 1908) or Dirichlet region (Dirichlet, 1850) by Delone). Delone used the convention of Bravais (1850) using the sides of the tetrahedron labeled by the symbols of the six Selling scalars. Figure 1 shows the labeling used in the International Tables for Crystallography (Henry & Lonsdale, 1952); Table 1 shows other choices that have been used. The contents for each type are described in Figure 1.

Burzlaff & Zimmermann (1985) revised the labeling of the types. Here we have returned to the numbering of the Bravais types to that of Delaunay (1932). In some cases, Delone included two forms within a single type. Burzlaff & Zimmermann (1985) renumbered by ordinals. We have labeled the Delone types that have multiple items as "A" and "B". Table 2 shows the various labelings. Figure 3 revises the figure of Delaunay (1932), using more modern notation. Table 1 lists the various labelings that have been used for the sides of the Bravais tetrahedron. Figure 1 shows the arrangement of the symbols as used in the International Tables for Crystallography.

<i>Delaunay (1932)</i>	<i>Henry & Lonsdale (1952)</i>	<i>Patterson & Love (1957)</i>	<i>Burzlaff & Zimmermann (1985)</i>	<i>Andrews et al. (2019b)</i>
g	P	h_{23}	$a_2.s_3$	s_1
k	R	h_{12}	$a_1.a_3$	s_3
l	S	h_{14}	$a_1.a_2$	s_4
m	T	h_{24}	$a_1.a_4$	s_5
h	Q	h_{13}	$a_2.a_4$	s_2
n	U	h_{34}	$a_3.a_4$	s_6

Table 1. The various terms used to describe the sides of the Bravais tetrahedron. (In the figures in Delaunay (1932) the tetrahedron has been rotated by -120 degrees)

(Delaunay, 1932)	(Burzlaff & Zimmermann, 1985)	this paper	
K_I	K1	C1	cI
K_{III}	K2	C3	cF
K_V	K3	C5	cP
Q_I	Q1	T1	tI
Q_{II}	Q2	T2	tI
Q_V	Q3	T5	tP
R_I	R1	H1	hR
R_{III}	R2	H3	hR
O_I	O1	O1A	oF
O_I	O2	O1B	oI
O_{II}	O3	O2	oI
O_{III}	O4	O3*	oI
O_{IV}	O5	O4	oS
O_V	O6	O5	oP
M_I	M1	M1A	mC
M_I	M2	M1B	mC
M_{II_2}	M3	M2A*	mC
M_{II}	M4	M2B*	mC
M_{III}	M5	M3	mC
M_{IV}	M6	M4	mP
T_I	T1	A1	aP
T_{II}	T2	A2*	aP
T_{III}	T3	A3*	aP
H_{IV}	H1	H4	hP

Table 2. *The 24 Delone types. (Delaunay, 1932)*

* not a full Bravais type.

2.2. The space \mathbf{S}^6

(Andrews *et al.*, 2019b) recast the Selling parameters to define a metric space, \mathbf{S}^6 .

The base vectors, \mathbf{a} , \mathbf{b} , \mathbf{c} of the unit cell are used to define $\mathbf{d} = -(\mathbf{a} + \mathbf{b} + \mathbf{c})$. A point s in \mathbf{S}^6 is defined as:

$$s = [s_1, s_2, s_3, s_4, s_5, s_6]$$

where $s_1 = \mathbf{b} \cdot \mathbf{c}$, $s_2 = \mathbf{a} \cdot \mathbf{c}$, $s_3 = \mathbf{a} \cdot \mathbf{b}$, $s_4 = \mathbf{a} \cdot \mathbf{d}$, $s_5 = \mathbf{b} \cdot \mathbf{d}$, and $s_6 = \mathbf{c} \cdot \mathbf{d}$.

2.3. Terminology of the Bravais lattice types

The Bravais tetrahedron symbol is described in Figure 1.

The different ways that the scalars have been labeled is shown in Table 1

The table of the Delone types is displayed in Figure 3. The table has been transposed from that of Delone. Where Delone listed 2 types in one cell, we have been split them into parts A and B. The crystal family names and abbreviations have been changed to modern usage.

2.4. Character

In S^6 for reduced cells, each Bravais type is a single, connected, origin-inclusive, Euclidean manifold. As such, all points in a particular manifold can be described by their “character”, a representation of the vectorsns of that type. The table of Delaunay (1932) included this information encoded in the formalism of Bravais, as a tetrahedron, with the sides marked to show which of the 6 Selling parameters were zero or which pairs (or multiplets) have equal values.

As an example, in Figure 2, the tetrahedron shows two zeros, in positions P and Q (s_1 and s_2). The slashes on the lines show that positions S and T (s_4 and s_5) are equal. This is encoded in the *character*, which is shown at the bottom of the item as (**00r sst**).

3. Algorithms for creation of an exhaustive list of the manifolds of the Bravais types

3.1. Deriving the projectors and perps

We will need to create projectors for each of the Bravais lattice types. The projectors will be used to generate images of probe points in each of the types, and the perps will measure the distance from each manifold.

We will use Selling reduction; Niggli reduction has a fundamental unit that is non-convex and some boundaries of the fundamental unit are partly closed and partly open (Andrews & Bernstein, 2014) leading to considerable complexity. Because Niggli

reduction divides the fundamental unit of Niggli reduction into separate all obtuse and all acute regions, the transitions between those are quite complex (Andrews & Bernstein, 2014). In space \mathbf{S}^6 (Andrews *et al.*, 2019*a*), the fundamental unit is the simple all-negative orthant of a 6-dimensional Cartesian space. Only two kinds of operations in the space will need to be considered: the 6 transform operations at the boundaries of the orthant (zeros of an axis) and 24 reflections (allowed permutations) (Andrews *et al.*, 2019*b*)

Twenty-four lattice types were enumerated by Delaunay (1932). Three of those are triclinic, and we will ignore them because all crystals can be indexed as triclinic. We shall need all representations of all non-triclinic lattice types within the \mathbf{S}^6 fundamental unit (all Selling-reduced cells) or those generated beyond the boundaries by boundary transforms. Three forms (M3, M2B, and O3) are reduced dimension boundaries that do not correspond to unique Bravais types; any lattice that falls in those three is indexed by one of the other types.

Seven of the 21 Delone types do not have a zero in their \mathbf{S}^6 representation; the presence of zero indicates that a form is on the boundary of the \mathbf{S}^6 fundamental unit. Since a point on the boundary transforms to another boundary point (Andrews *et al.*, 2019*a*), we can generate the Virtual Cartesian Point (VCP) (Andrews *et al.*, 2019*a*) appropriate to each zero in the \mathbf{S}^6 vector. Because the reduction operations do not commute, in the cases where there is more than one zero in the vector, all orderings of applying reductions to all of the zeros must be generated. (For example, for two zeros, there will be six vectors produced.) Again, there may be many duplicate results.

Finally, the projectors must be computed for each of the many sample vectors of the 21 types. We will also need the “perps”, the operators that give the normal vector to each such manifold. For a particular manifold, the projector applied to the probe gives the least-squares best fit point within that manifold to the probe vector. Perps

are computed by subtracting the corresponding projector from the unit matrix. The norm of a vector created by multiplying the probe times the projector is the distance from that manifold.

3.1.1. Generating sample vectors from all Bravais types

Step 1: Generate any random vector that contains no zero values and no duplicate values. For a later operation, it should only contain values large enough that adding or subtracting the smallest representable floating point number will not change the value in computer arithmetic (*DBL_MIN* in the C language). That value will be used to mark the positions of zeros in vectors that have been processed.

Step 2; For each Delone type, multiply its projector times the vector from Step 1. Store the resulting vector from Step 1 in a list with entries for each Bravais type (see Table 6 for the projectors).

Step 3:

a) If the vector result of Step 2 contains no zeros, generate the 24 reflections and store in the list by Bravais type.

LCA–need to normalize the vectors, just like in lattice matching. ? Can we use the lattice matching code here? This is very incomplete. The processing of multiple zeros is MISSING! But the use of DBL_MIN is there.

b) If the vector contains one zero, apply the boundary transform operation for that boundary to the vector, and store the products of the vector and its 24 reflections in the list. Note, this is where the choice of *DBL_MIN* has effect; adding or subtracting such a small value will not change any value except zero.

c) If the vector contains more than one zero and not *DBL_MIN*, first set one zero to *DBL_MIN*, and then return it to step b, using the modified vector. Then set the second zero to *DBL_MIN* (with the first zero still zero), and send that result to step

b. If there is a third zero, process it the same way as 2 zeros and return to c. (Note that no valid unit cell can have more than 3 zeros in space S^6 .)

Continue those steps until all the types have been processed. There will be duplicates within each type, which will be eliminated later.

3.1.2. Generate projectors from sample vectors

Each vector in each of the lists from the previous steps is a representative of one of the Delone types. Although a vector is a one-dimensional manifold, these vectors encode the information about the full manifolds of the Delone types in their zeros and their duplicate values. Now we discuss the creation of the projector matrices that correspond to each vector.

We begin by defining a function:

Fraction computes the reciprocal of the number of elements that equal an input value or zero if there are no duplicates.

LCA write pseudocode for Fraction.

The following steps will be repeated for each of the vectors in the list generated above in order to generate the list of the corresponding projector matrices.

To generate a matrix m starting from a vector.

Step 1: Zero any elements of the vector that have been set to DBL_MIN .

Step 2: For each of the six scalars

For i in 1-6 $m[i,i] = \{ \text{if } Fraction(s[i]) == 0.0 \text{ or } abs(s[i]) == 0.0 \} \text{ then } 0.0 \text{ else } Fraction(s[i])$

For i in 1-6 For j in 1-6 $m[i,j] = \{ \text{if } s[i]==s[j] \text{ or } abs(s[j]) > 0 \} \text{ then } Fraction(s[j]) \text{ else } 0.0$

Add m to a list of the projectors.

To finish, the duplicate projectors are removed within each type, leaving 239 non-

triclinic projectors. (If the triclinic cases are included, there are 10 more.) See Table 5.

3.2. Measuring the fit

When the library of projectors has been prepared, then the distance of any probe from each of the manifolds can be computed. The distance from the given manifold is just the norm of the perp for that manifold applied to the probe. An alternative, scale-free measure is the angle between the sample vector and its projected image.

4. Degenerate Delone types

Three of the 21 non-triclinic Delone types are only boundaries of other types. In Figure 4, Delone types M2B and M3 are in the row for orthorhombic, and O3 is in the row for rhombohedral and tetragonal. These types do not need to be searched for in general surveys. If a probe is close to one of these degenerate manifold, it will be close to one or both of the adjacent manifolds.

5. Verification

5.1. Rationale

Most of the proposals for Bravais lattice determination in the presence of experimental error do not have a clear proof that they are complete. For many years there were verbal complaints that available programs would not infrequently miss experimental cases (for example, TRACER (Lawton & Jacobson, 1965) and many anecdotal communications). To our knowledge, only the method of (Oishi-Tomiyasu, 2012) has clearly demonstrated completeness for exact values.

The justification that Sella is complete has three parts.

First: We require that the cell being tested be Selling reduced, and all Bravais lattice

types within the \mathbf{S}^6 fundamental unit (all \mathbf{S}^6 scalars negative) to have their projectors generated. Therefore, the 24 possible forms (reflections) of a reduced cell will be close to one of the 24 copies of the types. For the reflections, we do not need to consider the case of points near a boundary; the boundary transforms must be treated for that.

Second: In the case of the boundary transform operations, we take the case of a point that is infinitesimally distant from the manifold of a Bravais lattice type that has one zero in its scalars. Take the point in the manifold that is closest to the experimental point. We transform both by the corresponding boundary transform operation. We have generated a new pair of points in a different location, one of which is in some representation of the same Bravais lattice type. The points are still infinitesimally distant from each other.

Third: Assume we have a point that is outside the fundamental unit and is near an undiscovered manifold for a Bravais lattice type. If the point is near a boundary defined by a single zero, then we apply a boundary transform to the point and to the Bravais manifold, bringing them both into the fundamental unit. If all of the variations of all of the Bravais lattice types within and on the boundaries of the fundamental unit have been generated, then this putative undiscovered manifold has already been included in the list of possibilities. Similar arguments apply to the cases of two or three zeros.

If we apply all of the boundary transform operations to the representations of the Bravais lattice types, then there are no places that a point in the fundamental unit will fail to find the closest Bravais lattice (or lattices). As stated above, we found 239 non-triclinic possible representations.

What might occur if some reduced point has an unreduced copy near the all-negative orthant? Would it be possible for it to be close to one of the copies of one of the 21 Delone types? The reduced point is obviously in the non-positive orthant. Further,

because all possible copies of all of the Delone type manifolds have been generated, the reduced point will be near a copy of the manifold it was near when it was unreduced.

5.2. Testing against known cells

89539 unit cells were extracted from the Protein Data Bank in 2018 (Bernstein *et al.* (1977) and Berman *et al.* (2000)). When evaluated with Sella, all but 57 were found at zero distance from the described crystal class. The 57 were identified as incorrect unit cells for the assigned crystal class; however, the distances from the assigned classes were small because the deviations from the appropriate parameters were modest (see Table 3). The suspect cases have since been corrected (Burley, 2018).

PDB ID	Sp.Gr.	Delone type	distance (Å)	PDB ID	Sp.Gr.	Delone type	distance (Å)
1NUI	P3121	H4	0.0439	1SHN	P43212	T5	0.0491
2NW8	P3121	H4	0.0401	1C50	P43212	T5	1.9040
2J1L	P3121	H4	0.0307	2A1L	P43212	T5	0.0528
1VYI	P3121	H4	0.2504	1S2L	P43212	T5	0.0334
3FZ8	P32	H4	0.0575	1H9S	P41	T5	1.0149
2J5W	P3221	H4	0.0543	1H9R	P41	T5	1.0141
2VAM	P3221	H4	0.1166	2F0Q	P41	T5	0.0260
1Y8J	P3221	H4	0.0389	3EYU	P41	T5	0.0476
1F4V	P3221	H4	0.0276	1WV5	P41212	T5	0.0250
2ZP9	P6	H4	0.0528	2DF3	P41212	T5	0.0387
1DDR	P61	H4	0.0726	1L6O	P41212	T5	0.0346
1DDS	P61	H4	0.0726	3A58	P41212	T5	0.2976
1SGU	P61	H4	0.0295	2IU9	P41212	T5	0.0373
3CDC	P61	H4	0.0559	4BTP	P41212	T5	0.0666
2WAG	P6122	H4	0.0377	1W54	P4212	T5	0.0420
1LBM	P6122	H4	0.0312	2PBE	P42212	T5	0.0548
2O9Z	P62	H4	0.0402	3BR5	P42212	T5	0.2203
1ELZ	P6322	H4	0.4035	1GMD	P42212	T5	0.1400
1SA0	P65	H4	0.0681	1GMC	P42212	T5	0.1402
3KQI	P6522	H4	0.0331	2CCN	P42212	T5	0.0447
2F9Y	P6522	H4	0.0470	1CE1	P212121	O5	0.6472
3E73	P6522	H4	0.0523	3DQ2	P212121	O5	0.1058
3CAP	H3	H4	0.0586	1Z2A	P212121	O5	0.0670
2UX6	H32	H4	0.0386	2HA3	P212121	O5	0.3070
1ODT	H32	H4	0.0816	3BNJ	I4122	T2	0.9518
2FDI	P43	T5	0.0758	4MGP	I-42d	T1	0.2128
3HQ7	P43212	T5	0.2869	4ASL	C2221	O4	0.3383
1E2Q	P43212	T5	0.5482	3K7M	P432	C5	0.0517
				3GBN	I213	C1	1.2661

Table 3. 57 unit cells from the PDB around 2018 that did not match their types (later corrected)

5.3. Testing for continuity

The manifolds of the Bravais lattice types are characterized by required zeros of scalars and/or multiplets of equal values. For instance, all primitive monoclinic cells have two 90 degree angles and so require two zero scalars. Consider H1 as an example for multiplets. The character for H1 is (**rrr sss**); two triplets of equal values.

Consider the case of M4, primitive monoclinic, the character is (**00r stu**). For particular values for r,s,t,u, the best monoclinic cell will not depend on whatever values are substituted for the zeros. (It does not depend on the zero values because the projectors to that manifold create zero elements for any vector.) Imagine a plane with axis that are the values of the two elements of the character that are zero. Points in the plane represent unit cells with angles defined by the s_1 and s_2 and r,s,t,u. We can draw a circle in the s_1, s_2 plane, each point on the circle corresponding to a lattice.

Reducing the lattices corresponding to the points on the circle and r,s,t,u and calculating the distance of the reduced cell from (**00r stu**). Plotting the curve of the circle with the distance of each point from the origin changed to distance above will give a curve that should not have any discontinuities. See Figure 5.

Similarly, Bravais type O5 has a triplet of zeros, character (**000 rst**). Here we can generate a sphere that surrounds the orthorhombic point. See Figure 6.

Bravais type O4 (side-centered orthorhombic) has two zeros and a pair of required equal values, character (**00r sst**). The zeros can be treated the same as above for the case of M4 (primitive monoclinic). The pair of equal values must have an average value that remains equal to s in the lattice character. That means 3 values to vary (the 2 zeros and the distance from average value for the equal scalars), and we can create a sphere around the point (**00r sst**). See Figure 7.

6. Comparisons

LCA this section is incomplete. Table needs caption/label. Comparison to other distance measure; Data for other measures taken from Andrews & Bernstein (2014).

Lattice character	\mathbf{G}^6 distance	BGAOL Z score	XDS QI	Scaled QI	Sella
mP	20.138	0.657	1.0	0.13	1.06
oC	125.958	3.560	23.	8 3.09	13.82
mC	125.150	4.085	23.	4 3.03	13.80

Table 4. *Comparison of distance measures*

7. Interpreting the results

8. What could go wrong?

Acknowledgements Careful copy-editing and corrections by Frances C. Bernstein are gratefully acknowledged. Our thanks to Jean Jakoncic and Alexei Soares for helpful conversations and access to data and facilities at Brookhaven National Laboratory.

Funding information

Funding for this research was provided in part by: US Department of Energy Offices of Biological and Environmental Research and of Basic Energy Sciences (grant No. DE-AC02-98CH10886 ; grant No. E-SC0012704); U.S. National Institutes of Health (grant No. P41RR012408; grant No. P41GM103473; grant No. P41GM111244; grant No. R01GM117126, grant No. 1R21GM129570; grant No. P30GM133893); Dectris, Ltd.

References

- Andrews, L. C. & Bernstein, H. J. (2014). *J. Appl. Cryst.* **47**(1), 346 – 359.
 Andrews, L. C., Bernstein, H. J. & Sauter, N. K. (2019a). *Acta Cryst. A* **75**.
[Https://doi.org/10.1107/S2053273318015413](https://doi.org/10.1107/S2053273318015413).

- Andrews, L. C., Bernstein, H. J. & Sauter, N. K. (2019b). *Acta Cryst. A* **75**, 115 – 120.
- Berman, H. M., Westbrook, J., Feng, Z., Gilliland, G., Bhat, T. N., Weissig, H., Shindyalov, I. N. & Bourne, P. E. (2000). *Nucleic Acids Res.* **28**, 235 – 242.
- Bernstein, F. C., Koetzle, T. F., Williams, G. J. B., Meyer, Jr., E. F., Brice, M. D., Rodgers, J. R., Kennard, O., Shimanouchi, T. & Tasumi, M. (1977). *J. Mol. Biol.* **112**, 535 – 542.
- Bravais, A. (1850). *J. Ecole. Polytech.* pp. 1 – 128.
- Burley, S., (2018). Personal communication. Conversation about PDB unit cells.
- Burzlaff, H. & Zimmermann, H. (1985). *Z. Krist.-Crystalline Materials*, **170**(1-4), 247–262.
- Delaunay, B. N. (1932). *Z. Krist.* **84**, 109 – 149.
- Dirichlet, G. L. (1850). *J. reine angew. Math.* **40**, 209.
- Henry, N. F. M. & Lonsdale, K. (eds.) (1952). *International tables for X-ray Crystallography*, vol. I, Symmetry Groups, chap. 5.1 Reduction of General Primitive Reciprocal-lattice Triplet to the Corresponding Conventional Bravais-lattice Triplet, pp. 530 – 535. Kynoch Press.
- Lawton, S. L. & Jacobson, R. A. (1965). *The reduced cell and its crystallographic applications*. Tech. rep. .
- Niggli, P., (1928). Krystallographische und Strukturtheoretische Grundbegriffe, Handbuch der Experimentalphysik, Vol. 7, part 1. Akademische Verlagsgesellschaft, Leipzig.
- Oishi-Tomiya, R. (2012). *Acta Cryst. A* **68**(5), 525 – 535.
- Patterson, A. L. & Love, W. E. (1957). *Acta Cryst.* **10**(2), 111–116.
- Voronoi, G. (1908). *Journal für die reine und angewandte Mathematik*, **133**, 97–178. <Http://eudml.org/doc/149276>.
- Zimmermann, H. & Burzlaff, H. (1985). *Z. Kryst.* **170**, 241 – 246.

Table 5. The 21 non-triclinic Delone types with the count of representations. The asterisks indicate non-crystallographic types.

Delone type	Count
H4	12
C1	1
C3	3
C5	16
H1	4
H3	12
T1	3
T2	6
T5	48
O1A	3
O1B	1
O2	6
O3*	9
O4	36
O5	16
M1A	6
M1B	3
M2A	12
M2B*	12
M3*	18
M4	12

Table 6. Projectors for the 24 Delone types

C1	(cI)	[1 1 1 1 1 1 / 1 1 1 1 1 1 / 1 1 1 1 1 1 / 1 1 1 1 1 1 / 1 1 1 1 1 1 / 1 1 1 1 1 1]
C3	(cF)	[1 1 0 1 1 0 / 1 1 0 1 1 0 / 0 0 0 0 0 0 / 1 1 0 1 1 0 / 1 1 0 1 1 0 / 0 0 0 0 0 0]
C5	(cP)	[0 0 0 0 0 0 / 0 0 0 0 0 0 / 0 0 0 0 0 0 / 0 0 0 1 1 1 / 0 0 0 1 1 1 / 0 0 0 1 1 1]
T1	(tI)	[1 1 0 1 1 0 / 1 1 0 1 1 0 / 0 0 1 0 0 1 / 1 1 0 1 1 0 / 1 1 0 1 1 0 / 0 0 1 0 0 1]
T2	(tI)	[1 1 0 1 1 0 / 1 1 0 1 1 0 / 0 0 0 0 0 0 / 1 1 0 1 1 0 / 1 1 0 1 1 0 / 0 0 0 0 0 1]
T5	(tP)	[0 0 0 0 0 0 / 0 0 0 0 0 0 / 0 0 0 0 0 0 / 0 0 0 1 1 0 / 0 0 0 1 1 0 / 0 0 0 0 0 1]
H1	(hR)	[1 1 1 0 0 0 / 1 1 1 0 0 0 / 1 1 1 0 0 0 / 0 0 0 1 1 1 / 0 0 0 1 1 1 / 0 0 0 1 1 1]
H3	(hR)	[1 1 0 0 1 0 / 1 1 0 0 1 0 / 0 0 0 0 0 0 / 0 0 0 1 0 0 / 1 1 0 0 1 0 / 0 0 0 0 0 0]
H4	(hP)	[0 0 0 0 0 0 / 0 0 0 0 0 0 / 0 0 1 1 1 0 / 0 0 1 1 1 0 / 0 0 1 1 1 0 / 0 0 0 0 0 1]
O1A	(oF)	[1 1 0 1 1 0 / 1 1 0 1 1 0 / 0 0 1 0 0 0 / 1 1 0 1 1 0 / 1 1 0 1 1 0 / 0 0 0 0 0 1]
O1B	(oI)	[1 0 0 1 0 0 / 0 1 0 0 1 0 / 0 0 1 0 0 1 / 1 0 0 1 0 0 / 0 1 0 0 1 0 / 0 0 1 0 0 1]
O2	(oI)	[1 0 0 0 1 0 / 0 1 0 1 0 0 / 0 0 0 0 0 0 / 0 1 0 1 0 0 / 1 0 0 0 1 0 / 0 0 0 0 0 1]
O3	(oI)	[1 0 0 1 0 0 / 0 1 0 0 1 0 / 0 0 0 0 0 0 / 1 0 0 1 0 0 / 0 1 0 0 1 0 / 0 0 0 0 0 0]
O4	(oS)	[0 0 0 0 0 0 / 0 0 0 0 0 0 / 0 0 1 0 0 0 / 0 0 0 1 1 0 / 0 0 0 1 1 0 / 0 0 0 0 0 1]
O5	(oP)	[0 0 0 0 0 0 / 0 0 0 0 0 0 / 0 0 0 0 0 0 / 0 0 0 1 0 0 / 0 0 0 0 1 0 / 0 0 0 0 0 1]
M1A	(mC)	[1 1 0 0 0 0 / 1 1 0 0 0 0 / 0 0 1 0 0 0 / 0 0 0 1 1 0 / 0 0 0 1 1 0 / 0 0 0 0 0 1]
M1B	(mC)	[1 0 0 1 0 0 / 0 1 0 0 1 0 / 0 0 1 0 0 0 / 1 0 0 1 0 0 / 0 1 0 0 1 0 / 0 0 0 0 0 1]
M2A	(mC)	[1 0 0 1 0 0 / 0 1 0 0 1 0 / 0 0 0 0 0 0 / 1 0 0 1 0 0 / 0 1 0 0 1 0 / 0 0 0 0 0 1]
M2B	(mC)	[1 0 0 0 0 0 / 0 1 0 1 0 0 / 0 0 0 0 0 0 / 0 1 0 1 0 0 / 0 0 0 0 1 0 / 0 0 0 0 0 1]
M3	(mC)	[1 0 0 0 0 0 / 0 1 0 0 1 0 / 0 0 0 0 0 0 / 0 0 0 1 0 0 / 0 1 0 0 1 0 / 0 0 0 0 0 0]
M4	(mP)	[0 0 0 0 0 0 / 0 0 0 0 0 0 / 0 0 1 0 0 0 / 0 0 0 1 0 0 / 0 0 0 0 1 0 / 0 0 0 0 0 1]
A1	(aP)	[1 0 0 0 0 0 / 0 1 0 0 0 0 / 0 0 1 0 0 0 / 0 0 0 1 0 0 / 0 0 0 0 1 0 / 0 0 0 0 0 1]
A2	(aP)	[1 0 0 0 0 0 / 0 1 0 0 0 0 / 0 0 0 0 0 0 / 0 0 0 1 0 0 / 0 0 0 0 1 0 / 0 0 0 0 0 1]
A3	(aP)	[1 0 0 0 0 0 / 0 1 0 0 0 0 / 0 0 0 0 0 0 / 0 0 0 1 0 0 / 0 0 0 0 1 0 / 0 0 0 0 0 0]

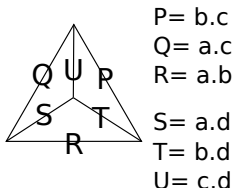


Fig. 1. Bravais tetrahedron with labeling as used in the International Tables

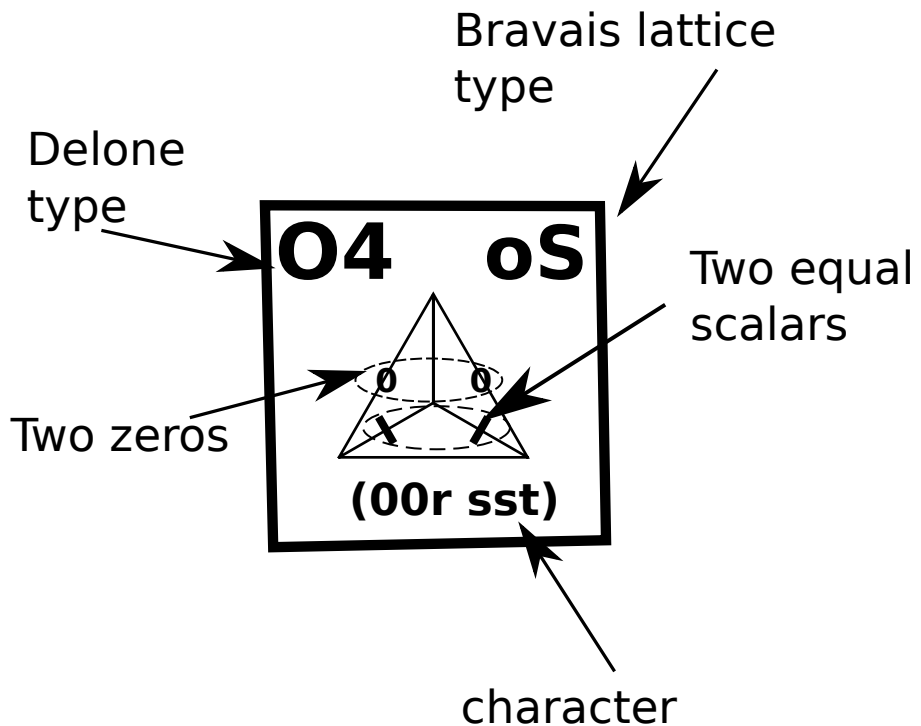
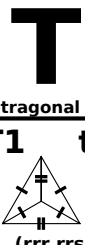
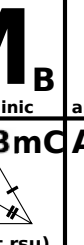
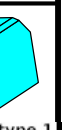
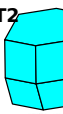
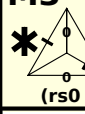
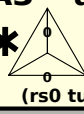
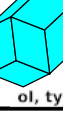
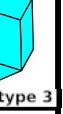
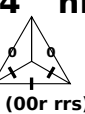
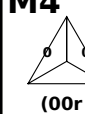
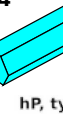
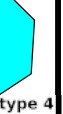
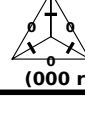
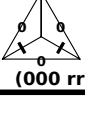
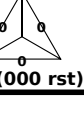


Fig. 2. The O4 item from the Delone Grid with Delone type description

Fig. 3. The Delone types

The Bravais Lattice Types

Lattice System

Fedorov Polyhedron Type	Lattice System									Dirichlet cells also known as Dirichlet domains Voronoi domains Fedorov parallelolohedra Wigner-Seitz cell
	C cubic	T tetragonal	H hexagonal (rhombohedral)	O _A orthorhombic	O _B orthorhombic	M _A monoclinic	M _B monoclinic	A anorthic		
1 truncated octahedron	C1 cl  (rrr rrr)	T1 tl  (rrr rrs)	H1 hR  (rrr sss)	O1A oF  (rrs rrt)	O1B ol  (rst rst)	M1AmC  (rrs ttu)	M1BmC  (rst rsu)	A1 aP  (rst uvw)	C1  cl, type 1	A1  aP, type 1
2 elongated dodecahedron		T2 tl  (rr0 rrs)		O2 ol  (rs0 srt)		M2AmC  (rs0 stu)	M2BmC  (rs0 rst)	A2 aP  (rs0 tuv)	M2A  mC, type 2	T2  tl, type 2
3 truncated octahedron	C3 cF  (rr0 rr0)		H3 hR  (rr0 sr0)	O3 ol  (rs0 rs0)		M3 mC  (rs0 ts0)		A3 aP  (rs0 tu0)	O3  ol, type 3	C3  cF, type 3
4 hexagonal prism			H4 hP  (00r rrs)	O4 oS  (00r sst)		M4 mP  (00r stu)			H4  hP, type 4	H4  hP, type 4
5 cuboid	C5 cP  (000 rrr)	T5 tP  (000 rrs)		O5 oP  (000 rst)				C5  cP, type 5	O5  oP, type 5	

*Not a full-dimensional Bravais type

O3 is a 2-D manifold between O2 and O1B

M3 is a 3-D manifold between M2A and M1B

M2B is a 3-D manifold between M1A and M1B

S6 Character

Each Bravais type has an associated S6 "character"

Each Character symbolically displays the pattern of unique, equal, or zero values for the type.

[modified after Delone, Galiulin, and Shtogrin, 1975]

Nullspace dimension	Free parameters							
5	1	C1 cl (rrr rrr)	C3 cF (rr0 rr0)	C5 cP(000 rrr)				
4	2	T1 tl (rrs rrs)	T2 tl (rr0 rrs)	T5 tp(000 rrs)	R1 hR (rrr sss)	R3 hR (rr0 sr0)	O3 ol (rs0 rs0)	H4 hp (00r rrs)
3	3	O1A oF (rrs rrt)	O2 ol (rs0 srt)	O4 oS (00r sst)	O5 oP (000 rst)	O1B ol (rst rst)	M3 mC (rs0 ts0)	M2B mC (rs0 rst)
2	4	M1A mC (rrs ttu)	M1B mC (rst rsu)	M2A mC (rs0 stu)	M4 mP (00r stu)	A3 aP (rs0 tu0)	*	
1	5	A2 aP (rs0 tuv)						
0	6	A1 aP (rst uvw)						

Fig. 4.

The red points indicate the original circle. The blue points are for the reduced cells.

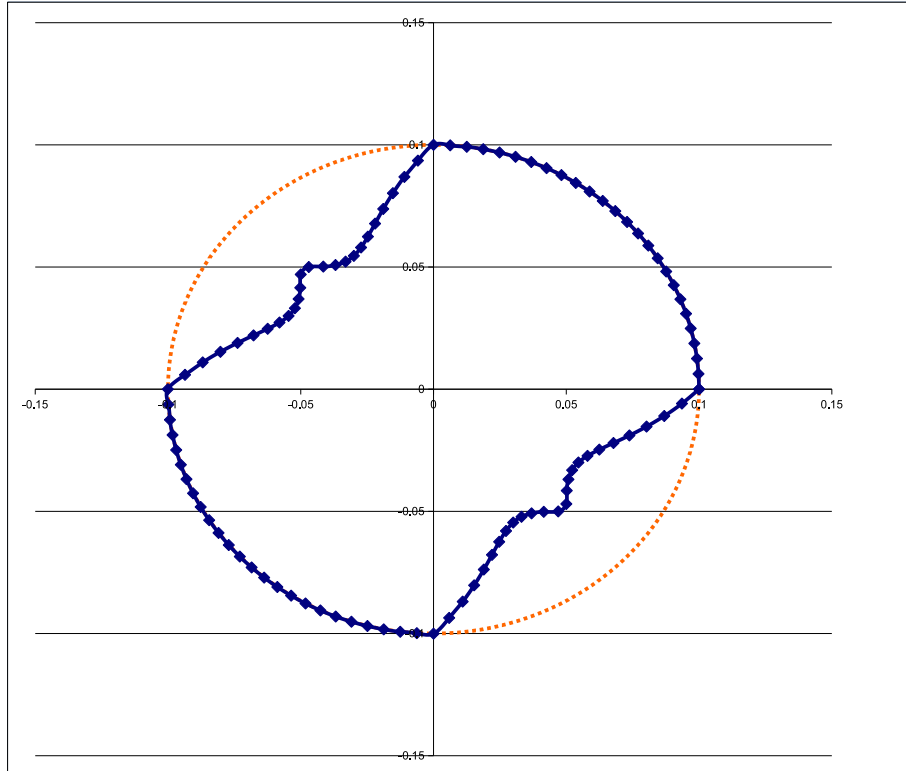


Fig. 5. Delone type M4: there are two zeros. A circle of 100 points with radius 0.1 is centered at 0,0. The lattices are reduced and the points are plotted at the distance from M4.

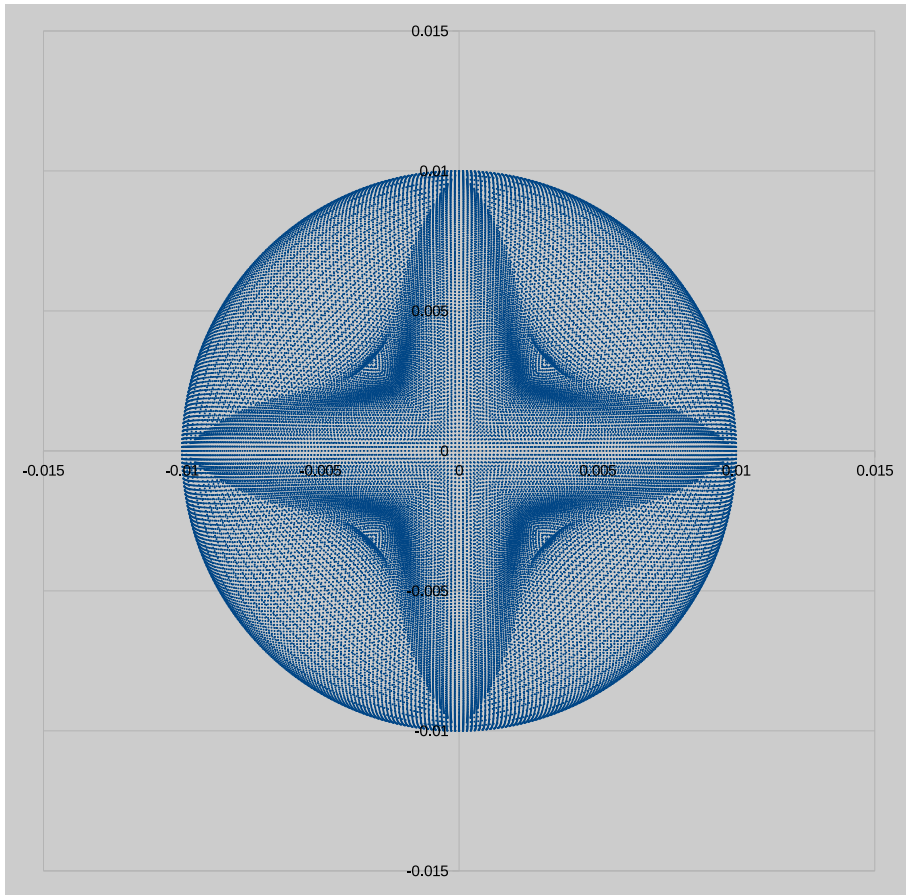


Fig. 6. Delone type O5: there are three zeros. A sphere is centered at 0,0,0, with radius 0.1. The lattices are reduced, and the point is placed at a distance equal to the distance from type O5. 50,000 points are plotted.

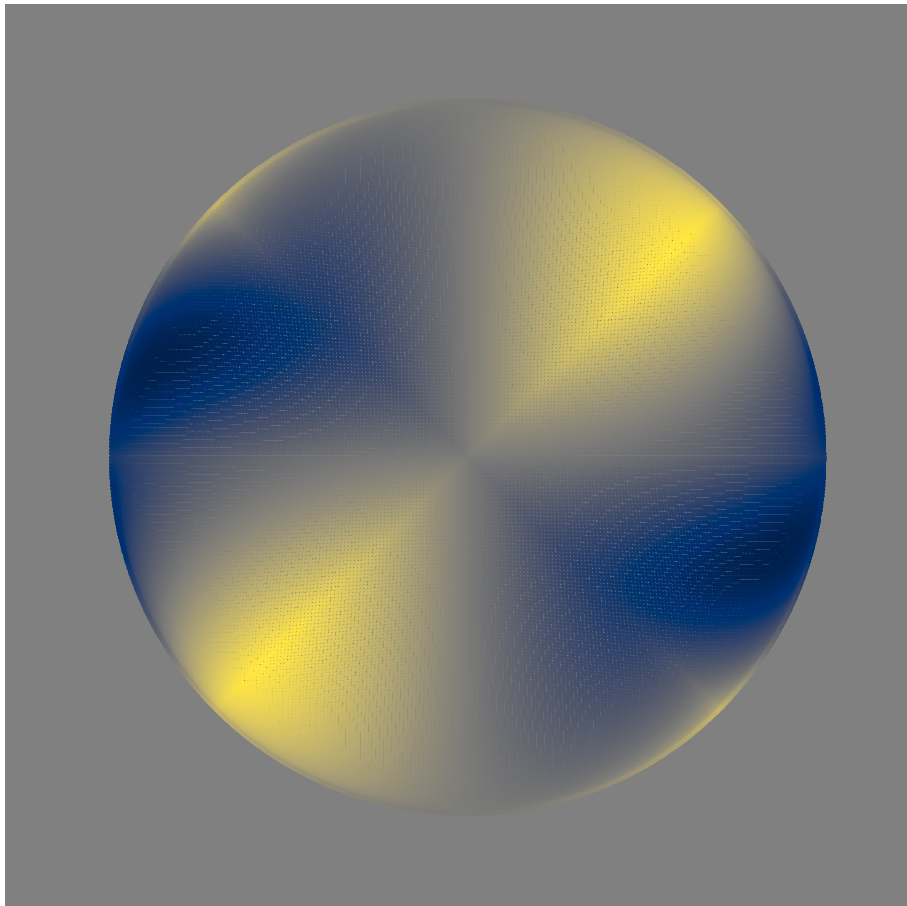


Fig. 7. Delone type O4: There are two zeros and one pair. A sphere with radius 0.1 was placed around one point. At each sphere point, the lattice was reduced and the point on the sphere was assigned a color (0.01) to blue (0.0075). 100,000 points are plotted.

Synopsis

A method for determining likely Bravais lattice types based on Selling (Delone) reduction. It is a complete, closed solution.
